IMPROVEMENT OF PARABOLIC NONLINEAR DISPERSIVE WAVE MODEL

By James M. Kaihatu[1]

ABSTRACT: Improvements to a previously published nonlinear parabolic wave model are developed and implemented. A second-order correction to a free-surface boundary condition used to develop the original model is formulated. The correction takes into account the complete second-order transformation between amplitudes of the velocity potential and those of the free-surface elevation. Additionally, wide-angle propagation terms are included in the model. It is shown that the model with the second-order correction retains the properties of third-order Stokes theory quite well in deep water. Comparisons of model behavior to data reveal that both nonlinearity and wide-angle propagation effects need to be included in the model for general wave transformation problems in shallow water. Skewness predictions are considerably improved by using both the second-order correction and by retaining a greater number of frequency components in the calculation. Asymmetry calculations are aided by incorporation of frequency-squared weighting for distribution of the dissipation function. Further improvement may entail a different form of the breaking model.

INTRODUCTION

For many nonlinear weakly dispersive wave transformation problems in shallow water, the Boussinesq equations of Peregrine (1967) or variants thereof (Freilich and Guza 1984; Liu et al. 1985; Herbers and Burton 1997) are used. The models are robust simulators of shallow water wave evolution so long as $kh \ll 1$, where k is a representative wave number and h a characteristic water depth. Much work has been done on increasing the dispersive range of weakly nonlinear models. Most of these developments can generally be divided into two classes: so-called "extended" Boussinesq models and nonlinear mild-slope equations [we are explicitly excluding nonlinear models with third-order Stokes nonlinearity, e.g., Kirby and Dalrymple (1983)]. The former class seeks to incorporate improved dispersive behavior by reformulation of the Boussinesq equations so that the linear dispersive properties mimic those of fully dispersive linear theory. These developments (and further enhancements) have been detailed extensively in several publications [e.g., Witting (1984), Madsen et al. (1991), Nwogu (1993), Schäffer et al. (1993), Schäffer and Madsen (1995), Wei et al. (1995), and Madsen and Schäffer (1998)].

In contrast to the extended Boussinesq equations, the nonlinear mild-slope equation models are fully dispersive linear models that incorporate second-order nonlinearity; they reduce to the linear mild-slope equation (Berkhoff 1972) in the linear limit. Bryant (1974) investigated the evolution of spatially periodic waves in time using equations with both second-order nonlinearity and fully dispersive coefficients over a flat bottom. The three-wave (triad) interaction terms are explicit due to the frequency domain formulation. Frequency dispersion effects served to detune the strength of the interaction, though Bryant (1974) demonstrated that significant energy exchange can still occur under conditions of near resonance. Agnon et al. (1993) and later Eldeberky and Madsen (1999) detailed deterministic 1D wave evolution models that contained full dispersion and triad interactions. Kaihatu and Kirby (1995) and Tang and Ouelette (1997) developed parabolic 2D extensions of the model of Agnon et al. (1993). These parabolic models, however, are limited to small aperture applications. Agnon and Sheremet (1997) and Eldeberky and Madsen (1999) developed stochastic variants of these nonlinear mild-slope equation models.

In the course of the model development, Eldeberky and Madsen (1999) noted that the models of Agnon et al. (1993), Kaihatu and Kirby (1995), and Agnon and Sheremet (1997) were somewhat incomplete in their formulations, since they used the first-order truncation of the dynamic free-surface boundary condition to move between amplitudes of ϕ (in terms of which the original problem was framed) and those of the free-surface elevation η, the desired dependent variable. Eldeberky and Madsen (1999) noted that the use of the first-order dynamic free-surface boundary condition in this transformation of variables led to underpredictions of energy transfer at higher frequencies. They used the full second-order free-surface boundary condition in this regard, but inverted the expression by successive approximations so that the full second-order model was expressed solely in terms of the amplitudes of η. They then developed both deterministic and stochastic models using this inverted expression.

In this study, we extend the models of Kaihatu and Kirby (1995) by the addition of wide-angle parabolic approximation terms and a second-order correction for the transformation from ϕ to η. The wide-angle parabolic approximation uses the results of Kirby (1986) to construct a nonlinear parabolic model with enhanced accuracy at wider angles of incidence to the onshore-offshore (x) coordinate axis. The second-order $\phi-\eta$ correction should ostensibly improve the simulation of wave propagation at high frequencies. The full second-order dynamic free-surface boundary condition is used to develop this second-order correction. We will investigate the effect of the addition of these terms on both monochromatic and spectral wave propagation over various bathymetries.

NONLINEAR MODEL OF KAIHATU AND KIRBY (1995)

The model analyzed here is the parabolic frequency-domain model of Kaihatu and Kirby (1995). The reader is referred to that publication for the full derivation. The model was derived starting from the boundary value problem for the velocity potential ϕ for water waves, expanded in Taylor series in ε ($=ka$, where k is wave number and a is a characteristic amplitude) about the still water level to second-order (retaining quadratic nonlinearity). The potential ϕ is a function of cross-shore coordinate x, longshore coordinate y, vertical coordinate z, and time t. We assume that the velocity potential has the form

$$\phi(x, y, z, t) = \sum_{n=1}^{N} f_n(z)\hat{\phi}_n(x, y)e^{-i\omega_n t} + \text{CC} \qquad (1)$$

where $\hat{\phi}_n$ is complex; CC denotes complex conjugate; N = total

[1]Oceanographer, Oc. Dyn. and Prediction Branch, Oceanography Div., Code 7322, Naval Res. Lab., Stennis Space Center, MS 39529-5004. E-mail: kaihatu@nrlssc.navy.mil

Note. Discussion open until September 1, 2001. To extend the closing date one month, a written request must be filed with the ASCE Manager of Journals. The manuscript for this paper was submitted for review and possible publication on January 19, 2000; revised August 7, 2000. This paper is part of the ***Journal of Waterway, Port, Coastal, and Ocean Engineering***, Vol. 127, No. 2, March/April, 2001. ©ASCE, ISSN 0733-950X/01/0002-0113–0121/$8.00 + $.50 per page. Paper No. 22159.

number of frequency components; the subscript n = frequency index, and

$$f_n(z) = \frac{\cosh k_n(h + z)}{\cosh k_n h} \tag{2}$$

Using the method of Smith and Sprinks (1975) on the boundary value problem and invoking resonant interaction theory (Phillips 1980) to select the interacting frequencies of a triad leads to a time-harmonic evolution equation for $\hat{\phi}_n$ with the triad nonlinearity explicitly detailed. Assuming a propagating wave form with a slowly varying amplitude

$$\hat{\phi}_n = -\frac{ig}{\omega_n} A_n e^{i\int k_n\, dx} \tag{3}$$

where A_n = complex amplitude; and ω = radian wave frequency, substituting this into the time-harmonic equation, and employing the parabolic approximation (Radder 1979) yields

$$2i(kCC_g)_n A_{nx} - 2(kCC_g)_n(\bar{k}_n - k_n)A_n + i(kCC_g)_{nx}A_n + [(CC_g)_n(A_n)_y]_y$$
$$= \frac{1}{4}\left(\sum_{l=1}^{n-1} RA_l A_{n-l} e^{i\int(k_l + \bar{k}_{n-l} - \bar{k}_n)dx} + 2\sum_{l=1}^{N-n} SA_l^* A_{n-l} e^{i\int(\bar{k}_{n-l} - \bar{k}_l - \bar{k}_n)dx}\right) \tag{4}$$

where R and S = complicated interaction coefficients [shown in equations 26 and 27 of Kaihatu and Kirby (1995)]; the subscripts x and y = differentiation with respect to that coordinate; C and C_g = phase and group speeds, respectively; and $\bar{k}_n$ = y-averaged wave number. The use of $\bar{k}_n$ is a consequence of the parabolic approximation; a phase redefinition is necessary. This is the model developed by Kaihatu and Kirby (1995, equation 35). The implicit Crank-Nicholson scheme (with iteration for the nonlinear terms) is used to solve (4). Implementation of the numerical scheme is similar to that detailed by Liu et al. (1985). One significant concern with the parabolic formulation (4) is the narrow aperture assumption used to develop the model. This precludes accurate modeling of obliquely incident waves.

For convenience we also write down the 1D version of (4)

$$A_{nx} + \frac{(kCC_g)_{nx}}{2(kCC_g)_n} A_n = -\frac{i}{8(kCC_g)_n}$$
$$\cdot\left(\sum_{l=1}^{n-1} RA_l A_{n-l} e^{i\int(k_l + k_{n-l} - k_n)dx} + 2\sum_{l=1}^{N-n} SA_l^* A_{n-l} e^{i\int(k_{n-l} - k_l - k_n)dx}\right) \tag{5}$$

where the wave numbers in the phase function revert to k_n. Eq. (5) is solved with a fourth-order Runge-Kutta technique coupled with an error-checking variable stepsize algorithm.

Eqs. (1) and (3) actually represent a transformation from amplitudes of ϕ to those of the free-surface η. This transformation is derived from

$$\phi_t + g\eta = 0 \tag{6}$$

This is the linearized form of the dynamic free-surface boundary condition at $z = 0$. Assuming time periodicity and the depth dependence in (2) yields the coefficient $-ig/\omega_n$ that multiplies the complex amplitude A_n in (3). In a sense, the first-order part of the amplitude of the free surface is being modeled with second-order nonlinearity with (4).

IMPROVEMENTS TO MODEL

Second-Order Relationship between η and ϕ

In this section we develop the second-order relationship between ϕ and η for use in the model of Kaihatu and Kirby (1995). We begin from the second-order nonlinear dynamic free-surface boundary condition

$$g\eta + \phi_t + \frac{1}{2}(\nabla_h\phi)^2 + \frac{1}{2}(\phi_z)^2 + \eta\phi_{zt} = O(\varepsilon^3); \quad z = 0 \tag{7}$$

We then use the lowest-order relationship [(6)], and substitute it into the fifth term in (7) to eliminate η. This leads to

$$\eta = -\frac{1}{g}\phi_t - \frac{1}{2g}(\nabla_h\phi)^2 - \frac{1}{2g}(\phi_z)^2 + \frac{1}{2g^2}(\phi_t)^2 \tag{8}$$

We then assume the following form for the amplitude of the free surface:

$$\eta = \sum_{n=1}^{N} B_n e^{i\int k_n\, dx - \omega_n t} + \text{CC} \tag{9}$$

Substituting (9), (1), and (3) into (7), enforcing resonant triad interaction among frequency components, and incorporating the phase redefinition inherent in the parabolic approximation yields

$$B_n = A_n - \frac{1}{4g}$$
$$\cdot\left(\sum_{l=1}^{n-1} IA_l A_{n-l} e^{i\int(k_l + \bar{k}_{n-l} - \bar{k}_n)dx} + 2\sum_{l=1}^{N-n} JA_l^* A_{n+l} e^{i\int k_{n+l} - \bar{k}_l - \bar{k}_n dx}\right) \tag{10}$$

where

$$I = \omega_l^2 + \omega_l\omega_{n-l} + \omega_{n-l}^2 - g^2\frac{k_l k_{n-l}}{\omega_l\omega_{n-l}} \tag{11}$$

$$J = \omega_l^2 - \omega_l\omega_{n+l} + \omega_{n+l}^2 - g^2\frac{k_l k_{n+l}}{\omega_l\omega_{n-l}} \tag{12}$$

This is the second-order correction to the relation between amplitudes of ϕ and those of η. Eq. (4) would remain the primary evolution model, but the above equation would be used whenever the free surface is needed. As with (5), the $\bar{k}_n$ revert to k_n for 1D propagation.

Wide-Angle Parabolic Model

The parabolic approximation inherently limits the model application to a small range of wave approach angles about the offshore (x) coordinate. Several researchers have incorporated wide-aperture corrections into parabolic models (Booij 1981; Kirby 1986). Kirby (1986) investigated the scaling involved in developing the higher-order parabolic approximation. He determined that the appropriate dynamic balance between nonlinearity, bottom slope magnitude, and the modulation scale for diffraction is entirely arbitrary. For his case, Kirby chose the dynamic balance between the modulation length scale $\tilde{\delta}$, the nonlinearity ε, and the bottom slope parameter $\tilde{\mu}$ to be $\tilde{\delta}^2 \sim \varepsilon \sim \mu^{1/2}$. He then noted that at $O(\tilde{\delta}^4\varepsilon)$ nonlinear terms and bottom slope terms appear at the same order. Using this choice of scales, he derived the wide-angle linear parabolic model over a flat bottom, with bottom slope and nonlinear terms simply added to the resulting equation. Employing the same choice of scaling allows us to add the nonlinear triad terms to the model of Kirby (1986) without currents. The resulting model is

$$2i(kCC_g)_n A_{nx} - 2(kCC_g)_n(\bar{k}_n - k_n)A_n + i(kCC_g)_{nx}A_n$$
$$+ \left(\frac{3}{2} + \frac{\bar{k}_n}{2k_n}\right)[(CC_g)_n A_{ny}]_y$$
$$- \frac{i}{2}\left[\frac{k_{nx}}{k_n^2} + \frac{(kCC_g)_{nx}}{2(k^2CC_g)_n}\right][(CC_g)_n A_{ny}]_y + \frac{i}{k}[(CC_g)_n A_{ny}]_{yy}$$
$$= \frac{1}{4}\left[\sum_{l=1}^{n-1} RA_l A_{n-l} e^{i\int(\bar{k}_l + \bar{k}_{n-l} - \bar{k}_n)dx} + 2\sum_{l=1}^{N-n} SA_l^* A_{n-l} e^{i\int(\bar{k}_{n-l} - \bar{k}_l - \bar{k}_n)dx}\right] \tag{13}$$

The correspondence to (4) is apparent. This model also utilizes (10) as the higher-order correction.

PERMANENT FORM SOLUTIONS

In this section we investigate the ability of the models to replicate properties of deep and shallow water periodic waves. Different methods have been used in various studies to confirm model behavior, particularly in deep water (Bryant 1974; Tang and Ouelette 1997; Eldeberky and Madsen 1999). In this section we examine asymptotic model behavior by developing numerical permanent form solutions of the model equations, following Kirby (1991). This is somewhat more convenient than analytical means (Bryant 1974) because of the two-equation system implemented [(5) and (10)].

We formulate the permanent form solution by redefining the time-harmonic velocity potential and free-surface elevation. Thus we use

$$\phi(x, y, z, t) = \sum_{n=1}^{N} \frac{-ig}{2\omega_n} f_n(z)\tilde{a}_n e^{i\int n(k_1+\tilde{k})\,dx - \omega_n t} + \text{CC} \tag{14}$$

$$\eta(x, y, t) = \sum_{n=1}^{N} \tilde{b}_n e^{i\int n(k_1+\tilde{k})\,dx - \omega_n t} + \text{CC} \tag{15}$$

instead of (1) with (3), and (9), respectively. In this case k_1 is the linear wave number for the base frequency ω_1, and $\tilde{k}$ is the distortion to the linear wave number due to nonlinear effects. This form of the phase function assumes that all harmonics of the wave move at the same speed, and thus amplitude dispersion is necessary.

Use of (14) and (15) in (5) and (10) requires the following substitutions:

$$A_n = \tilde{a}_n e^{\int [n(k_1+\tilde{k})-k_n]\,dx} \tag{16}$$

$$B_n = \tilde{b}_n e^{\int [n(k_1+\tilde{k})-k_n]\,dx} \tag{17}$$

Substituting (16) and (17) into (5) and (10), respectively, and assuming no change in energy flux (as would be the case for a propagating permanent-form wave) we obtain the following set of algebraic equations:

$$[n(k_1+\tilde{k}) - k_n]\tilde{a}_n + \frac{1}{8\omega_n C_{gn}}\left(\sum_{l=1}^{n-1} R\tilde{a}_l\tilde{a}_{n-l} + 2\sum_{l=1}^{N-n} S\tilde{a}_l\tilde{a}_{n+l}\right) = 0 \tag{18}$$

$$\tilde{b}_n = \tilde{a}_n + \frac{1}{4g}\left(\sum_{l=1}^{n-1} I\tilde{a}_l\tilde{a}_{n-l} + 2\sum_{l=1}^{N-n} J\tilde{a}_l\tilde{a}_{n+l}\right) \tag{19}$$

We wish to find a set of $\tilde{a}_n$ and a wave-number distortion $\tilde{k}$ that satisfies (18) for any specified wave height H, wave period T, water depth h, and number of harmonics N. We need one more equation. From the definition of wave height as being the distance from crest to trough

$$H = 2\sum_{n=1,3,5\ldots}^{N} \tilde{b}_n = 2\sum_{n=1,3,5\ldots}^{N} \cdot\left[\tilde{a}_n + \frac{1}{4g}\left(\sum_{l=1}^{n-1} I\tilde{a}_l\tilde{a}_{n-l} + 2\sum_{l=1}^{N-n} J\tilde{a}_l\tilde{a}_{n+l}\right)\right] \tag{20}$$

Eqs. (18) and (20) are solved via the Newton-Raphson method to double precision. Eq. (19) is then used to convert $\tilde{a}_n$ to $\tilde{b}_n$. Finding the permanent-form solution without the second-order effect in the $\phi-\eta$ transformation would entail neglecting the nonlinear summations in (20).

We first compare the phase speeds from the permanent-form solutions (both with and without the second-order correction) with those from the Stokes third-order theory. The Stokes third-order theory is the lowest-order Stokes theory to include the effects of nonlinear amplitude dispersion, and as such serves as a fair test of the nonlinear dispersion characteristics of the model. Bryant (1974) suggested that the solutions to equations similar to those detailed here match the Stokes third-order theory in deep water for small ε. To show the effect of the size of ε, we use several initial wave heights in the permanent-form solution. For each fixed wave height, we vary the water depth and calculate the associated permanent-form solution. We use $T = 5$ s and $N = 10$, and vary the water depth from $h = 20$ m to $h = 9$ m. We used wave heights of 0.5, 1.0, 2.0, and 3.0 m. These correspond to $\varepsilon = 0.04$, 0.08, 0.16, and 0.24 at $h = 20$ m. The resulting phase-speed comparisons (plotted as a function of kh, where the k is from linear dispersion) are shown in Fig. 1. It is evident that, in general, all solutions compare very well to the third-order Stokes theory from deep to intermediate water, with the smaller wave-height solutions (smaller ε) comparing best. Additionally, it appears that the second-order correction has little effect on the phase speed.

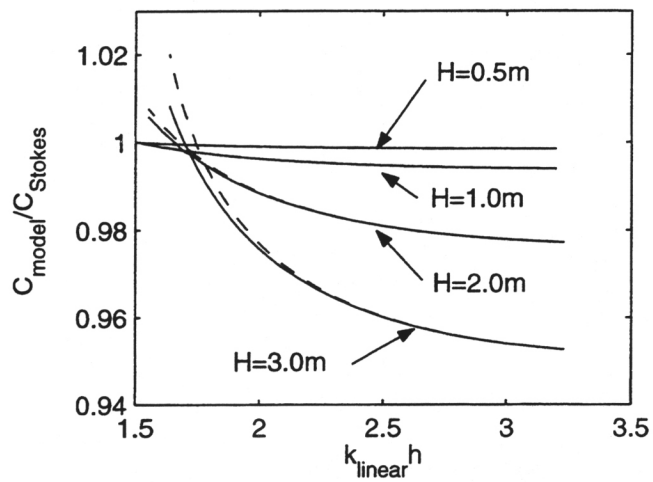

FIG. 1. Comparison of Phase Speed from Corrected and Uncorrected Permanent-Form Solutions to Third-Order Stokes Theory ($T = 5$ s and $N = 10$ with H and kh Varying; Solid = Permanent-Form Solution of Model with Second-Order Correction; Dashed = Permanent-Form Solution of Model without Second-Order Correction)

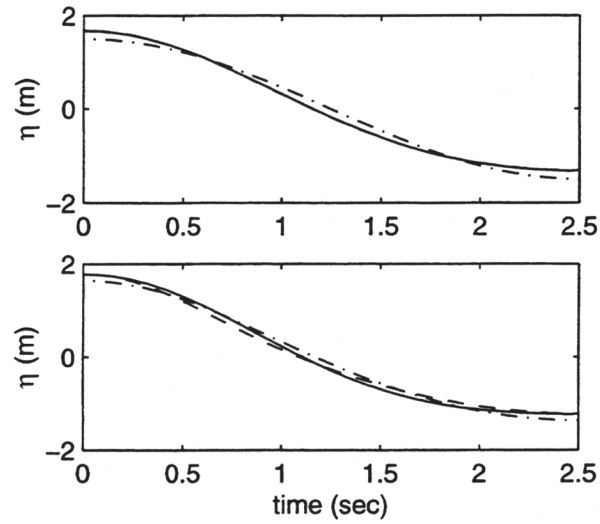

FIG. 2. Comparison of Free Surface Profiles from Corrected and Uncorrected Permanent-Form Solutions to Third-Order Stokes Theory: (a) $h = 20$ m; (b) $h = 9$ m ($T = 5$ s, $H = 3$ m, and $N = 10$; Solid = Third-Order Stokes Theory; Dashed = Permanent-Form Solution of Model with Second-Order Correction; Dash-Dot = Permanent-Form Solution of Model without Second-Order Correction)

We also compare the free-surface realizations from the permanent-form solutions to the third-order Stokes theory at h = 20 m and h = 9 m. This comparison is shown in Fig. 2. The h = 20 m case reveals that the permanent-form solution with the second-order correction matches both Stokes third-order theory quite well, while the solution without the correction does not. Both solutions diverge somewhat from the Stokes theory with h = 9 m. This is to be expected, as the Stokes theory becomes invalid with decreasing kh (shallower water depth). It is clear that inclusion of the second-order correction is essential for the proper free-surface solution.

We now perform a similar analysis to the shallow water behavior of the permanent-form solution. We use the stream function theory (Dean 1965) as our baseline for comparison, as it is a numerical solution of the full boundary value water wave problem. We specifically employ 15th-order stream function theory, as this should retain enough terms in the Fourier series solution to suppress Gibbs' oscillations. We first investigate the accuracy of the phase-speed calculation. For the permanent-form solutions (with and without the second-order correction) we use T = 10 s, H = 0.1, and N = 15, and vary the depth from h = 10 m to h = 1 m. This varies μ^2 = 0.40 to μ^2 = 0.04. The relevant nonlinear parameter in classical weakly-dispersive shallow water wave theory is δ (=a/h) rather than ε. The chosen wave conditions and range of water depths lead to δ = 0.005 at h = 10 m and δ = 0.05 at h = 1 m. The Ursell number $U_r = \delta/\mu^2$ thus ranges from 0.012 to 1.25, essentially spanning the range from intermediate to shallow water for weak nonlinearity. The resulting comparison of phase speed from the permanent-form solutions to stream function theory is shown in Fig. 3. The phase speeds from the permanent-form solutions compare very well with those from stream function theory. Additionally, the second-order correction has little effect on the phase-speed calculation. Comparison of the resulting free-surface profiles at h = 10 m and h = 1 m is shown in Fig. 4. Agreement is excellent, with the second-order correction again having little effect. This is in agreement with Eldeberky and Madsen (1999), who suggested that the second-order correction becomes less important as $kh \rightarrow 0$.

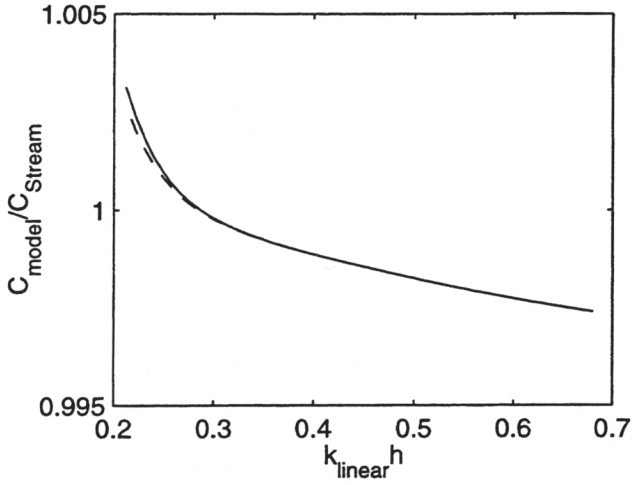

FIG. 3. Comparison of Phase Speed from Corrected and Uncorrected Permanent-Form Solutions to 15th-Order Stream Function Theory (T = 10 s, H = 0.1 m, and N = 15 with varying kh; Solid = Permanent-Form Solution of Model with Second-Order Correction; Dashed = Permanent-Form Solution of Model without Second-Order Correction)

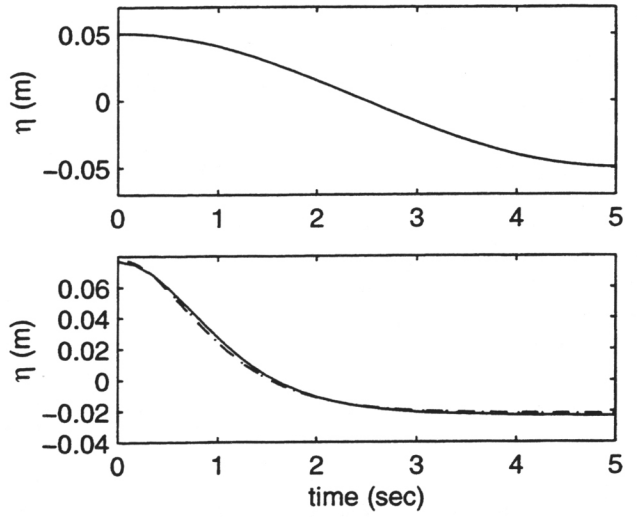

FIG. 4. Comparison of Permanent-Form Solutions to 15th-Order Stream Function Theory: (a) h = 10 m; (b) h = 1 m (H = 0.1 m and T = 10 s; Solid = 15th-Order Stream Function Theory; Dashed = Permanent-Form Solution of Model with Second-Order Correction; Dash-Dot = Permanent-Form Solution of Model without Second-Order Correction)

COMPARISON WITH LABORATORY DATA

In this section we conduct some comparisons to laboratory data. This was also done by Kaihatu and Kirby (1995) but we extend the range of testing to cases in greater relative depth.

Circular Shoal over Flat Bottom

Chawla (1995) conducted wave transformation experiments in the directional wave basin of the Center for Applied Coastal Research at the University of Delaware. The bathymetry consisted of a flat bottom with a circular shoal. The experimental layout with gauge transects is shown in Fig. 5. The constant water depth away from the shoal is h = 0.45 m, and the depth over the top of the shoal is h = 0.08 m. Both monochromatic and irregular directional wave conditions were run in the tank; we investigate the monochromatic case here. The experiment was also described in Chawla et al. (1998).

We examine the case of a monochromatic wave with T = 1 s and H = 0.0233 m. A spatial resolution $\Delta x = \Delta y$ = 0.06 m was used; this is substantially finer than required for reliable model results. We compare the nonlinear narrow-angle [(4)], and nonlinear wide-angle [(13)] models to the data. We also use a linear wide-angle model (Kirby 1986) to gauge the effect of the inclusion of nonlinearity. For the nonlinear models we use a permanent-form solution with the wave parameters above. This wave condition has ε = 0.049 and μ^2 = 3.58, a deep water condition with very low nonlinearity. It was not

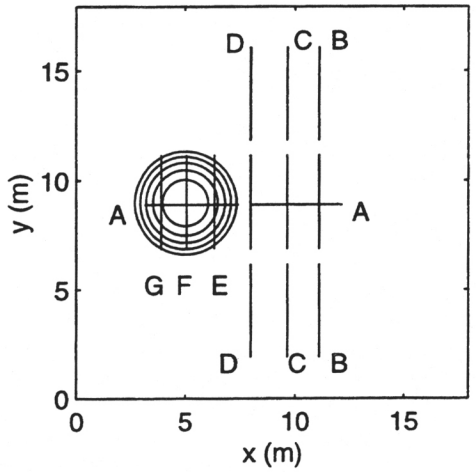

FIG. 5. Layout of Experiment of Chawla (1995) (Letters Refer to Gauge Transects; Waves Propagate from Left to Right)

clear initially what the proper value of N should be for best simulating this experiment. To investigate this, data from a gauge located in the focal region of the experiment (the area of greatest wave height, near $x = 7$ m and $y = 9$ m) were analyzed. This region is where the energy exchange, if present, would be greatest. The analysis (not shown) revealed that the amplitudes of the second and third harmonics are one and two orders of magnitude smaller, respectively, than that of the primary harmonic. Using $N = 2$ kept 92% of the variance at this gauge. Subsequent tests with $N = 3$ revealed little difference.

Figs. 6 and 7 show the comparison of wave heights (normalized by the incident wave height) from the uncorrected nonlinear models and the linear model to data at four gauge transects. Addition of the second-order correction had virtually no effect, and so those results are not shown. In general, the addition of nonlinearity improved the fit between data and model. Amplitude dispersion effects are evident over the top of the shoal (transect A-A in Fig. 6); the linear model overpredicts the wave height along that transect. The addition of the wide-angle propagation correction does have a significant effect, perhaps more so than nonlinearity. This is most evident along transects B-B, C-C, and D-D (Figs. 6 and 7). Both the linear and nonlinear wide-angle models capture the diffraction fringes seen in the data, while the narrow-angle nonlinear model does not appear to move energy sufficiently fast along the longshore (y) axis. To better quantify the fit to data we make use of the "index of agreement" (Wilmott 1981) for each transect

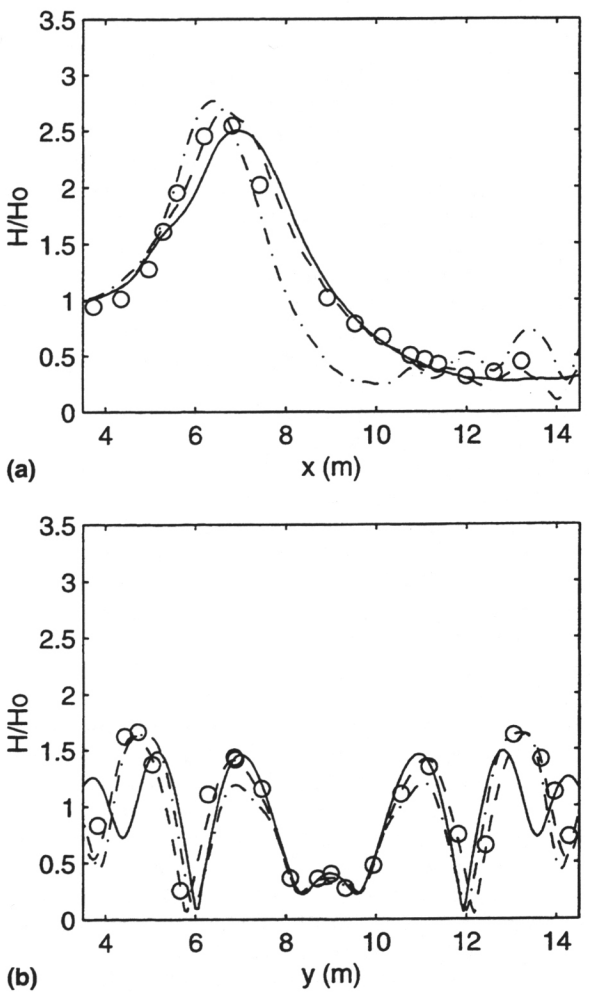

FIG. 6. Comparison of Models to Data of Chawla (1995): (a) Gauge Transect A-A; (b) Gauge Transect B-B [Solid Line = Eq. (4); Dashed Line = Eq. (13); Dash-Dot = Linear Wide-Angle Parabolic Model; Open Circles = Data of Chawla (1995)]

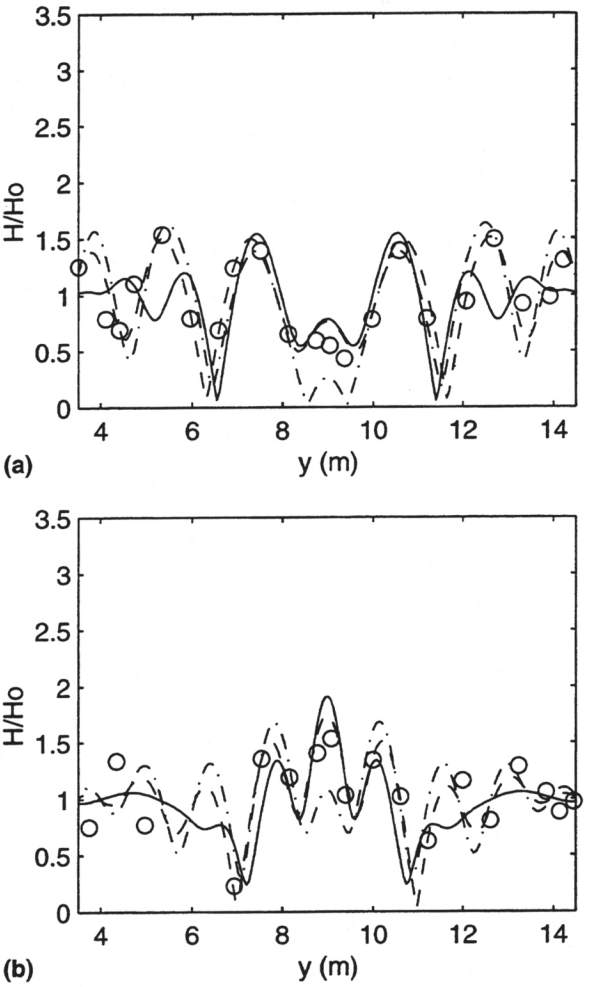

FIG. 7. Comparison of Models to Data of Chawla (1995): (a) Gauge Transect C-C; (b) Gauge Transect D-D [Solid Line = Eq. (4); Dashed Line = Eq. (13); Dash-Dot = Linear Wide-Angle Parabolic Model; Open Circles = Data of Chawla (1995)]

$$I_a = 1 - \frac{\sum_{j=1}^{J} [y(j) - x(j)]^2}{\sum_{j=1}^{J} [|y(j) - \bar{x}| + |x(j) - \bar{x}|]^2} \tag{21}$$

where J = total number of data points in each transect; $x(j)$ = data; $y(j)$ = predicted values from the models; and $\bar{x}$ = data averaged along each transect. The index I_a varies from 0 (complete disagreement) to 1 (complete agreement). The resulting values of I_a are shown in Table 1. Of the seven transects, the nonlinear model with wide-angle terms [(13)] does best along four (A-A, B-B, C-C, and E-E) and thus best overall. The linear wide-angle model does best along one transect (G-G) and second-best along two (C-C and E-E). The narrow-angle nonlinear model [(4)] does best along transects D-D and F-F.

TABLE 1. Index of Agreement I_a for Model Comparisons to Data of Chawla (1995)

Transect (1)	Linear wide-angle model (2)	Eq. (4) (3)	Eq. (13) (4)
A-A	0.9700	0.9892	0.9948
B-B	0.8908	0.7816	0.9755
C-C	0.8453	0.6891	0.9325
D-D	0.6510	0.9258	0.8734
E-E	0.9913	0.9686	0.9924
F-F	0.9550	0.9614	0.9564
G-G	0.6469	0.6209	0.6259

The relatively poor agreement exhibited by the wide-angle models along D-D may be due to the error exhibited in the prediction of the diffraction pattern. Slight misplacement of the diffraction patterns relative to those in the data may be penalized heavily in the I_a metric. On the other hand, the narrow-angle model exhibits significantly less oscillation, which appears to yield better values of I_a along this transect. Nevertheless, the wide-angle models overall do qualitatively replicate the diffraction lobes seen in the data along D-D, while the narrow-angle model does not.

Random Wave Shoaling

Mase and Kirby (1993) performed an experiment in which irregular waves were transformed over a sloping bottom. One of the cases run used a Pierson-Moskowitz-type spectrum with a peak frequency $f_p = 1$ Hz in water depth of 0.47 m, leading to a kh at the peak of almost two. This is a demanding test for most nonlinear wave models; shallow water Boussinesq models overshoal most of the frequency range. The offshore root-mean-square wave height H_{rms} is 0.0454 m. The experimental setup and gauge placement is shown in Fig. 8.

There is significant wave breaking in this experiment; the highest waves break near the wave gauge at $h = 0.175$ m. To simulate energy loss due to wave breaking in this experiment, Kaihatu and Kirby (1995) augmented the 1D model [(5)] with a dissipation term (Mase and Kirby 1993); the completed model is

$$A_{nx} + \frac{(kCC_g)_{nx}}{2(kCC_g)_n} A_n + \alpha_n A_n = -\frac{i}{8(kCC_g)_n} \cdot \left[\sum_{l=1}^{n-1} RA_l A_{n-l} e^{i\int (k_l + k_{n-l} - k_n)\,dx} + 2 \sum_{l=1}^{N-n} SA_l^* A_{n+l} e^{i\int (k_{n+l} - k_l - k_n)\,dx} \right] \quad (22)$$

where α_n = frequency-weighted dissipation distribution

$$\alpha_n = \alpha_{n0} + \left(\frac{f_n}{f_{\text{peak}}} \right)^2 \alpha_{n1} \quad (23)$$

$$\alpha_{n0} = F\beta(x) \quad (24)$$

$$\alpha_{n1} = [\beta(x) - \alpha_{n0}] \frac{f_{\text{peak}}^2 \sum_{n=1}^{N} |A_n|^2}{\sum_{n=1}^{N} f_n^2 |A_n|^2} \quad (25)$$

where f_{peak} = peak frequency; and $\beta(x)$ = probabilistic function of Thornton and Guza (1983). The free parameter F in (24) serves as a weighting that determines the split between an f_n^2-weighted dissipation and a frequency-independent dissipation. Kirby and Kaihatu (1997) and Chen et al. (1997) provide theoretical and experimental support for $F = 0$, which allows only f_n^2-weighted dissipation.

Kaihatu and Kirby (1995) demonstrated that the model with dissipation [(22)] agreed very well with the data of Mase and Kirby (1993). They used $N = 300$ for the calculations (up to

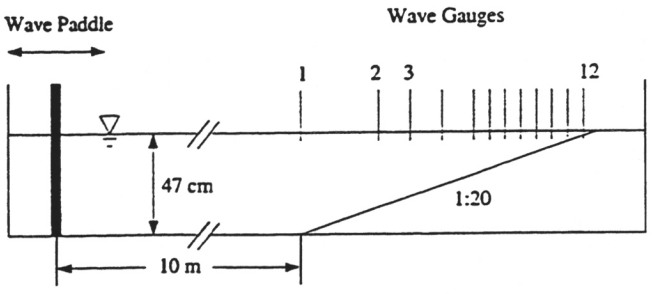

FIG. 8. Layout of Experiment of Mase and Kirby (1992)

≈3 Hz), retaining around 93% of the total variance in the wavefield. Best results for the spectral comparisons were obtained with $F = 0.5$. Later, Kaihatu and Kirby (1997) investigated comparisons between model and the data of Mase and Kirby (1993) using higher-order moments (skewness, asymmetry) as metrics. In a shoaling wavefield, skewness would be expected to increase (as nonlinearity increases) and asymmetry become more negative (as wave crests become pitched forward). They noted that these higher-order moments were often underpredicted, even though the spectra comparisons revealed excellent agreement. They found that retaining more frequency components (up to the Nyquist limit) increased the accuracy of these predictions. Since skewness and asymmetry are measures that involve the surface shape, inclusion of higher-frequency components tend to improve the details of the free surface (flatter troughs, more peaked crests) even if little energy is present.

Eldeberky and Madsen (1999) demonstrated the effect of the retained second-order terms in the $\phi-\eta$ transformation by comparing their model with the Mase and Kirby (1993) data. They showed model-data comparisons of wave spectra from their stochastic model [augmented by the frequency-independent dissipation mechanism of Eldeberky and Battjes (1996)] to those from the model of Agnon and Sheremet (1997), with improved results. Eldeberky and Madsen (1999) also showed that skewness of the wave field was better predicted in the nonbreaking region than that from the model of Agnon and Sheremet (1997). However, predictions of asymmetry were quite poor; they were in fact positive for most of the domain. This lack of negative asymmetry is likely more a consequence of the dissipation distribution used in their breaking model than the exact form of the nonlinearity. Kaihatu and Kirby (1997) showed that neglecting frequency weighting of the dissipation (a choice equivalent to $F = 1$) leads to asymmetry predictions that almost never become negative inside the domain, a clear indication that the waves are not attaining a "pitched forward" shape characteristic of surf zone waves.

In this study, we investigate the effect of the second-order transformation correction on the evolution of the spectra and the higher-order moments (skewness, asymmetry) in the experiment of Mase and Kirby (1993). We first run the model [(22)], using $N = 300$. This was done both with and without the second-order correction [(10)]. We use $F = 0.5$ for the uncorrected model, and $F = 0.5$ and $F = 0$ for the corrected model; this latter step is done to investigate the effect of the full f_n^2 weighting on the results. Fig. 9 shows comparisons at a few locations in the domain; they are typical of the comparisons at the other gauges. It is clear that the correction has almost no effect on the evolution of the spectral density for frequencies <1.7 Hz, a limit that corresponds to $kh = 5.8$ at the wavemaker. In the frequency range beyond $f = 1.7$ Hz, there is some (though little) improvement from the second-order correction. Additionally, the use of $F = 0$ affects the resulting spectra predictions only slightly.

Fig. 10 shows comparisons of skewness and asymmetry from the models to the data (also truncated at 300 frequency components). Here the effect of the second-order correction is clear. The uncorrected model greatly underpredicts the skewness in the unbroken region ($h > 0.175$ m) but climbs upward in the breaking region. The corrected model with $F = 0.5$ exhibits the opposite trend: skewness is better resolved in the nonbreaking region but drops off dramatically in accuracy in the breaking region. However, this model appears to do best overall for skewness. The corrected model with $F = 0$ has a skewness prediction trend similar to that of $F = 0.5$ for the nonbreaking region, with a greater falloff in accuracy in the breaking region. Asymmetry is somewhat poorly predicted by all models in the breaking zone, though improved over that of

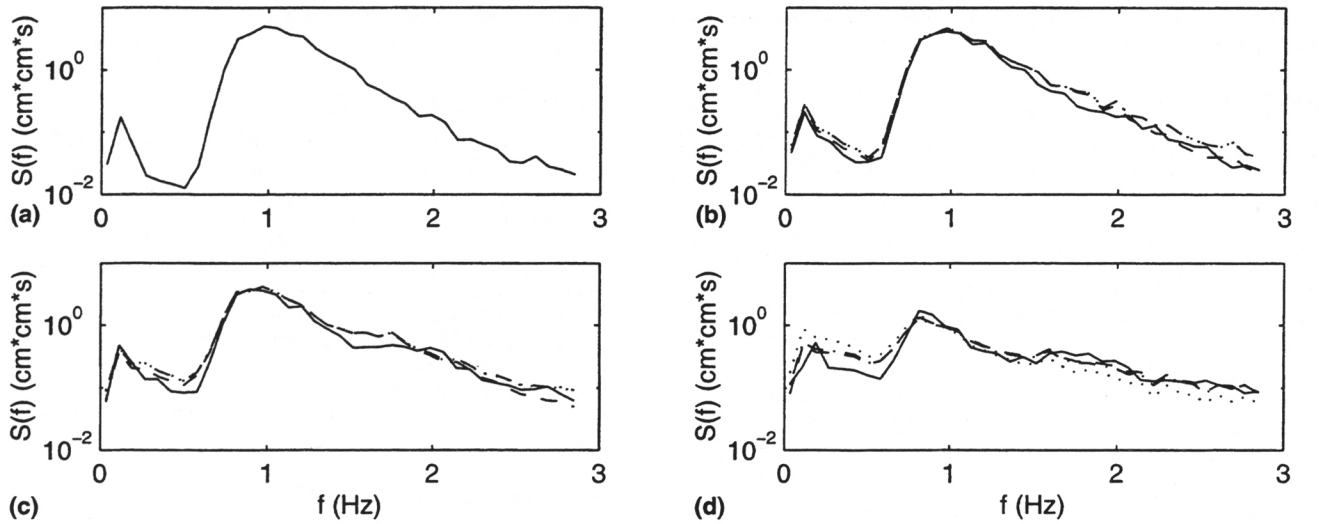

FIG. 9. Comparison of Wave Spectra from Model to Data of Mase and Kirby (1992), $N = 300$: (a) $h = 0.47$ m; (b) $h = 0.20$ m; (c) $h = 0.125$ m; (d) $h = 0.05$ m [Solid Line = Data of Mase and Kirby (1992); Dashed Line = Eq. (22); Dash-Dot = Eq. (22) with Second-Order Correction, Eq. (10) and $F = 0.5$. Dotted = Eq. (22) with Second-Order Correction, Eq. (10) and $F = 0$]

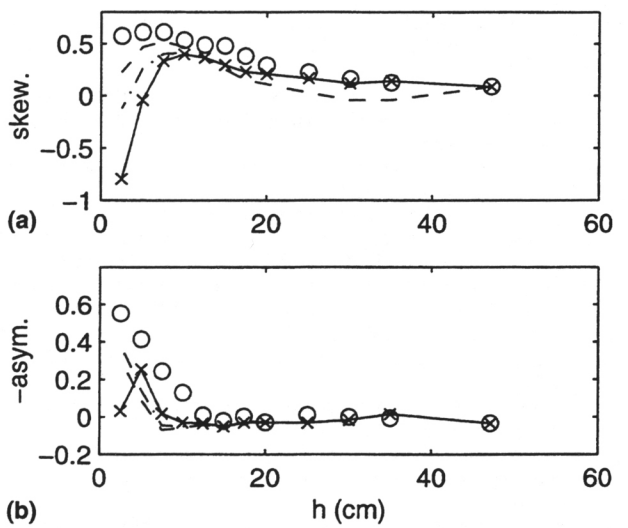

FIG. 10. Comparison of Skewness and (Negative) Asymmetry, $N = 300$: (a) Skewness; (b) Negative Asymmetry [Open Circles = Data of Mase and Kirby (1992); Solid Line = Eq. (22) with Second-Order Correction, Eq. (10), and $F = 0.5$; Dashed Line = Eq. (22) and $F = 0.5$; Dash-x = Eq. (22) with Second-Order Correction, Eq. (10) and $F = 0$]

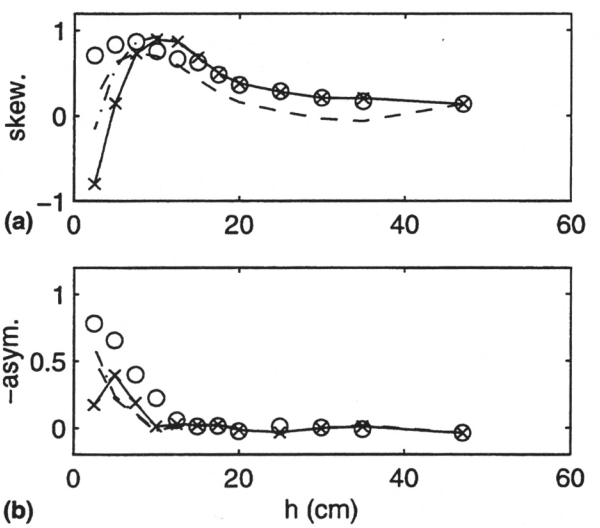

FIG. 11. Comparison of Skewness and (Negative) Asymmetry, $N = 500$: (a) Skewness; (b) Negative Asymmetry [Open Circles = Data of Mase and Kirby (1992); Solid Line = Eq. (22) with Second-Order Correction, Eq. (10) and $F = 0.5$; Dashed Line = Eq. (22) and $F = 0.5$; Dash-x = Eq. (22) with Second-Order Correction, Eq. (10) and $F = 0$]

Eldeberky and Madsen (1999) in that negative values of asymmetry do result. The corrected model with $F = 0$ fares best in asymmetry prediction with the sole exception of the shallowest gauge. Generally, the lack of better agreement in asymmetry may be due to the form (rather than just the frequency distribution) of the breaking model than the nonlinearity. Kirby and Kaihatu (1997) showed that the steepness-triggered eddy viscosity dissipation model included in the time-domain extended Boussinesq model of Wei et al. (1995) predicted the skewness and asymmetry values of the Mase and Kirby (1993) data set very well, including the final gauge. This eddy viscosity formulation is equivalent to $F = 0$, and thus difficulty at the final gauge is not an indictment of this value of F. Incorporating a frequency-domain version of this dissipation into the present model may improve the asymmetry values relative to that predicted by a bulk energy dissipation model such as that used here. We note that asymmetry is reliably modeled for depths $>h = 0.15$ m.

To investigate the effect of higher values of N on the third-moment statistics, we rerun the simulations using $N = 500$ (maximum frequency of 5 Hz). Fig. 11 shows the skewness and asymmetry results with $N = 500$ for both data and models. Here again it is clear that the second-order correction does improve the skewness. Fig. 11(a) shows the skewness reliably modeled up to $h = 0.15$ m with the corrected model. Again, as with $N = 300$, the corrected model with $F = 0.5$ fares best. On the other hand, asymmetry [shown in Fig. 10(b)] is again not helped by retention of the second-order correction, though good agreement with data is evidenced up to $h = 0.15$ m and negative asymmetries do result in the surf zone. Additionally, the corrected model with $F = 0$ shows the best comparison, again with the exception of the shallowest gauge. It is also apparent that skewness and (negative) asymmetry values for both model and data are increased relative to the $N = 300$ case. Overall, it appears that the effect of the second-order correction is more evident in calculation of higher-order moments (particularly skewness) than in comparisons of spectra except for the highest frequencies. The inclusion of the second-order correction is generally an improvement for third moment statistics for any given N, with further improvements evident as

N increases. Using $F = 0$ generally aids the asymmetry calculations.

CONCLUSIONS

In this study we develop two improvements to the nonlinear parabolic mild-slope equation model of Kaihatu and Kirby (1995), shown here in (4). The first is a second-order correction to a transformation used in the original model to move between amplitudes of ϕ and those of η [(10)]. The lack of consideration of this second-order correction was noted by Eldeberky and Madsen (1999) as being potentially damaging to accurate energy transfer at high frequencies. The second improvement is the addition of wide-angle propagation terms to the original model, using the formalism of Kirby (1986) to develop the final wide-angle parabolic model [(13)].

Investigation of the model behavior at deep and shallow water asymptotes was done by development and analysis of a permanent-form solution to the model. The permanent-form solution was developed from the evolution equations, resulting in (18) and (20), with the nonlinear terms in (20) deactivated to simulate neglect of the second-order correction [(10)]. The phase speeds from the permanent-form solutions compare favorably with the Stokes third-order theory, particularly for small values of wave height (small ε), with the second-order correction not affecting the results significantly. However, the free-surface comparisons showed that the second-order correction is necessary for a good match to the Stokes theory in deep water. The shallow water asymptotic behavior of the permanent-form solutions was compared with stream function theory (Dean 1965), with favorable results for both free surface in shallow water, and phase speed over a range of kh. In this asymptotic case, the second-order correction had almost negligible effect.

Comparisons with two laboratory data sets were then performed. The wide-angle linear model and the narrow- and wide-angle nonlinear models [(4) and (13), respectively] were first compared with the circular shoal experiment data of Chawla (1995). The effect of the inclusion of the wide-angle propagation terms are evident, more so than the inclusion of nonlinearity. To help sort out model performance, the "index of agreement" (Wilmott 1981) was used. This confirmed the superior performance of the wide-angle nonlinear model [(13)] relative to the other models.

The final test was a comparison to the irregular wave shoaling experiment of Mase and Kirby (1993). A dissipation mechanism was included in the model. The frequency dependence of this mechanism is split into an f_n^2-weighted distribution and a frequency-independent portion. The parameter F controlled the split, with $F = 0$ being entirely f_n^2 weighted and $F = 1$ entirely frequency independent. The model with dissipation [(22)] was run with $F = 0.5$ [determined by Kaihatu and Kirby (1995) as the best fit to the data] and $F = 0$, both with and without the second-order correction. The effects of the inclusion of this correction and the value of F became more obvious when calculating third moments (skewness, asymmetry). Using $N = 300$, we showed that the skewness is better predicted in the nonbreaking ($h > 0.175$ m) portion of the experiment with the correction applied. Wave asymmetry, on the other hand, does not show any improvement with the correction, though applying both the correction and $F = 0$ aids considerably. Negative values of asymmetry (corresponding to a forward-pitched wave train) do result, however, an improvement over Eldeberky and Madsen (1999), who used the equivalent of $F = 1$. Simulations with $N = 500$, along with the inclusion of the second-order correction, greatly improves the accuracy of the skewness results relative to $N = 300$. Asymmetry, however, is still poorly predicted. Again, the model with the correction and $F = 0$ helps with asymmetry predictions. Further improvement of third moment calculations would probably require new formulations of the dissipation model.

ACKNOWLEDGMENTS

This study was supported by the Office of Naval Research through two projects: the Naval Research Laboratory 6.2 Core project "Coastal Simulation," and the National Ocean Partnership Program project entitled "Development and Verification of a Comprehensive Community Model for Physical Processes in the Nearshore Ocean." Drs. Arun Chawla (now of Center for Coastal and Land Margin Research, Oregon Graduate Institute of Science and Technology) and James T. Kirby (Center for Applied Coastal Research, University of Delaware) supplied the circular shoal data. Discussions with Dr. Jayaram Veeramony (Center for Ocean and Atmospheric Modeling, University of Southern Mississippi) helped greatly. Comments from anonymous reviewers improved the initial submitted version of the paper. This is NRL contribution number JA/7322-00-0008; distribution unlimited.

APPENDIX. REFERENCES

Agnon, Y., and Sheremet, A. (1997). "Stochastic nonlinear shoaling of directional spectra." *J. Fluid Mech.*, Cambridge, U.K., 345, 79–100.

Agnon, Y., Sheremet, A., Gonsalves, J., and Stiassnie, M. (1993). "Nonlinear evolution of a unidirectional shoaling wave field." *Coast. Engrg.*, 20, 29–58.

Berkhoff, J. C. W. (1972). "Computation of combined refraction-diffraction." *Proc., 13th Int. Conf. Coast. Engrg.*, ASCE, New York, 471–490.

Booij, N. (1981). "Gravity waves on water with non-uniform depth and current." *Rep. 81-1*, Dept. Civ. Engrg., Delft University of Technology, Delft, The Netherlands.

Bryant, P. J. (1974). "Stability of periodic waves in shallow water." *J. Fluid Mech.*, Cambridge, U.K., 66, 81–96.

Chawla, A. (1995). "Wave transformation over a submerged shoal." MS thesis, Dept. of Civ. Engrg., University of Delaware, Newark, Del.

Chawla, A., Özkan-Haller, H. T., and Kirby, J. T. (1998). "Spectral model for wave transformation and breaking over irregular bathymetry." *J. Wtrwy., Port, Coast., and Oc. Engrg.*, ASCE, 124(4), 189–198.

Chen, Y., Guza, R. T., and Elgar, S. (1997). "Modeling spectra of breaking surface waves in shallow water." *J. Geophys. Res.*, 102, 25035–25046.

Dean, R. G. (1965). "Stream function representation of nonlinear ocean waves." *J. Geophys. Res.*, 70, 4561–4572.

Eldeberky, Y., and Battjes, J. A. (1996). "Spectral modeling of wave breaking: Application to Boussinesq equations." *J. Geophys. Res.*, 101, 1253–1264.

Eldeberky, Y., and Madsen, P. A. (1999). "Deterministic and stochastic evolution equations for fully-dispersive and weakly nonlinear waves." *Coast. Engrg.*, 38, 1–24.

Freilich, M. H., and Guza, R. T. (1984). "Nonlinear effects on shoaling surface gravity waves." *Philosophical Trans. Royal Soc.*, London, A311, 1–41.

Herbers, T. H. C., and Burton, M. C. (1997). "Nonlinear shoaling of directionally spread waves on a beach." *J. Geophys. Res.*, 102, 21101–21114.

Kaihatu, J. M., and Kirby, J. T. (1995). "Nonlinear transformation of waves in finite water depth." *Phys. of Fluids*, 7(8), 1903–1914.

Kaihatu, J. M., and Kirby, J. T. (1997). "Effects of mode truncation and dissipation on predictions of higher order statistics." *Proc., 25th Int. Conf. Coast. Engrg.*, ASCE, New York, 123–136.

Kirby, J. T. (1986). "Higher-order approximations in the parabolic equation method for water waves." *J. Geophys. Res.*, 91, 933–952.

Kirby, J. T. (1991). "Intercomparisons of truncated series solutions for shallow water waves." *J. Wtrwy., Port, Coast., and Oc. Engrg.*, ASCE, 117(2), 143–155.

Kirby, J. T., and Dalrymple, R. A. (1983). "A parabolic model for the combined refraction-diffraction of Stokes waves by mildly varying toography." *J. Fluid Mech.*, Cambridge, U.K., 136, 453–466.

Kirby, J. T., and Kaihatu, J. M. (1997). "Structure of frequency domain models for random wave breaking." *Proc., 25th Int. Conf. Coast. Engrg.*, ASCE, New York, 1144–1155.

Liu, P. L.-F., Yoon, S. B., and Kirby, J. T. (1985). "Nonlinear refraction-diffraction of waves in shallow water." *J. Fluid Mech.*, Cambridge, U.K., 153, 185–201.

Madsen, P. A., Murray, R., and Sørensen, O. R. (1991). "A new form of the Boussinesq equations with improved linear dispersion characteristics." *Coast. Engrg.*, 15, 371–388.

Madsen, P. A., and Schäffer, H. A. (1998). "Higher-order Boussinesq-

type equations for surface gravity waves: Derivation and analysis." *Philosophical Trans. Royal Soc.*, London, A356, 3123–3184.
Mase, H., and Kirby, J. T. (1993). "Hybrid frequency-domain KdV equation for random wave transformation." *Proc., 23rd Int. Conf. Coast. Engrg.*, ASCE, New York, 474–487.
Nwogu, O. (1993). "Alternative form of Boussinesq equations for near-shore wave propagation." *J. Wtrwy., Port, Coast., and Oc. Engrg.*, ASCE, 119(6), 618–638.
Peregrine, D. H. (1967). "Long waves on a beach." *J. Fluid Mech.*, Cambridge, U.K., 27, 815–827.
Phillips, O. M. (1980). *The dynamics of the upper ocean*, Cambridge University Press, London.
Radder, A. C. (1979). "On the parabolic equation method for water-wave propagation." *J. Fluid Mech.*, Cambridge, U.K., 95, 159–176.
Schäffer, H. A., and Madsen, P. A. (1995). "Further enhancements of Boussinesq-type equations." *Coast. Engrg.*, 26, 1–14.
Schäffer, H. A., Madsen, P. A., and Deigaard, R. (1993). "A Boussinesq model for wave breaking in shallow water." *Coast. Engrg.*, 20, 185–202.
Smith, R., and Sprinks, T. (1975). "Scattering of surface waves by a conical island." *J. Fluid Mech.*, Cambridge, U.K., 72, 373–384.
Tang, Y., and Oulette, Y. (1997). "A new kind of nonlinear mild-slope equation for combined refraction-diffraction of multifrequency waves." *Coast. Engrg.*, 31, 3–36.
Thornton, E. B., and Guza, R. T. (1983). "Transformation of wave height distribution." *J. Geophys. Res.*, 88, 5925–5938.
Wei, G., Kirby, J. T., Grilli, S. T., and Subramanya, R. (1995). "A fully nonlinear Boussinesq model for surface waves. I: Highly nonlinear, unsteady waves." *J. Fluid Mech.*, Cambridge, U.K., 294, 71–92.
Wilmott, C. J. (1981). "On the validation of models." *Phys. Geography*, 2, 219–232.
Witting, J. M. (1984). "A unified model for the evolution of nonlinear water waves." *J. Computational Phys.*, 56, 203–236.